Climate Dynamics (2019) 52:6719–6733
https://doi.org/10.1007/s00382-018-4539-y

Transient contributions to the forcing of the atmospheric annual cycle

A diagnostic study with the DREAM model

Nicholas M. J. Hall[1] · Stephanie Leroux[2] · Tercio Ambrizzi[3]

Received: 15 June 2018 / Accepted: 14 November 2018 / Published online: 19 November 2018

Abstract
The forcing of the global circulation is examined using a primitive equation model and a 38-year reanalysis dataset. One-timestep integrations are initialised with selected sets of initial conditions, and the forcing budget for the mean annual cycle is deduced. This budget consists of sources and sinks of momentum, temperature and humidity which are balanced by dynamical terms. The associated timescale interactions are examined in detail. The time-mean forcing is balanced by time-mean fluxes, annual cycle interactions and transient fluxes. The annual cycle of the forcing is balanced by the interaction of annual cycle anomalies with the time-mean flow and with themselves (this latter cycle-cycle interaction term is found to be important for the moisture supply over West Africa). Transient interactions on other timescales also contribute to the forcing of the annual cycle, but the interaction term between the annual cycle and other timescales is small, as is the storage term associated with seasonal tendencies. This objectively derived empirical forcing is then used to drive the dynamical model. The resulting simple GCM is called DREAM (Dynamical Research Empirical Atmospheric Model). This is the first time this approach has been used with an annual cycle. The systematic errors of DREAM compared to the reanalysis chiefly concern the momentum balance in the southern hemisphere jet. Perpetual season simulations are similar to individual seasons from the annual cycle run, consistent with the small seasonal tendency term in the forcing.

Keywords Annual Cycle · Dynamical model · DREAM · Simple GCM

1 Introduction

The regular sinusoidal displacement of the sun between the tropics forces a cyclic response in the state of the global atmosphere. The signal is so strong that we often seek to eliminate it to reveal signals on other timescales, dubbed 'interannual' or 'intraseasonal'. But since the atmosphere-ocean system contains damping, nonlinearity and scale interaction, the observed annual cycle is not a simple function of the orbital forcing. It will contain variations in amplitude, phase and frequency depending on the location and the variable considered (note that here we refer to the 'annual cycle' as the annually repeating component of all the variability, not just a single frequency component).

It has long been recognised that different physical contributions to the annual cycle display differing seasonality. For example, the contribution of the ocean heat transport varies greatly with season (Oort and Vonder Haar 1976) and has a phase lag of 3–4 months from the solar forcing (Levitus 1984). Phase lags depend on location and differ for annual and semi-annual components (Hsu and Wallace 1976; White and Wallace 1978). There is also considerable seasonal variation in stationary wave and transient activity (Oort 1971). A comprehensive budget based on a combination of data sources and reanalysis was presented by Fasullo and Trenberth (2008a, b). They concentrated on sources of uncertainty, especially in the surface fluxes, but also highlighted the predominant influence of land-sea contrast in determining geographical variations in the annual cycle. Atmosphere-ocean coupling can impinge on the annual cycle, especially in the East Pacific (Horel 1982; Wang 1994; Xie 1994; Liu 1996; Chen and Jin 2017). Nonlinear dynamical phenomena

✉ Nicholas M. J. Hall
Nick.Hall@legos.obs-mip.fr

[1] LEGOS, 14 Ave. Edouard Belin, 31400 Toulouse, France

[2] OceanNext, MEOM, Grenoble, France

[3] IAG, University of Sao Paulo, Sao Paulo, Brazil

such as land-sea advection (McKinnon et al. 2013) and wave dissipation (Kerr-Munslow and Norton 2006; Jucker and Gerber 2017) are also implicated. Huang and Sardeshmukh (2000) showed that the semi-annual component of the atmosphere's angular momentum is largely a nonlinear response to the annual component of the forcing. Some of the physical mechanisms that determine the annual cycle also act on other timescales, and as discussed by Wu et al. (2008) one might consider that the annual cycle does not repeat exactly from one year to the next. The problem of separating the annual cycle from other timescales is thus a physical and dynamical problem, was well as an exercise in data analysis.

In a modelling context, if the annual cycle is viewed as a response to forcing, then the partition between what constitutes the forcing and what constitutes the response will depend on the scope and complexity of the model. For example, an atmosphere-only model will respond to insolation and sea surface temperature (Sud et al. 2002; Biasutti et al. 2003). In a nonlinear system, these physically distinct contributions can interact. So a budget for the variance associated with the annual cycle must include extra interaction terms. In a similar way, the forcing of the annual cycle also depends on dynamically distinct interaction terms on other timescales. Fluxes due to transient variations contribute not only to the forcing of the mean flow, but also to the annual cycle, and variations on seasonal timescales can also interact with one another to modify the annual cycle. The way in which the dynamical budget is partitioned between these timescale interactions can be diagnosed from a long time series of reanalysis data using a dynamical model. A general budget derived in this manner may be instructive when interpreting variability in atmospheric GCMs and simpler models.

The first goal of this paper is thus to present a novel method for deriving a comprehensive budget for the forcing of the annual cycle using a primitive equation model as a diagnostic tool. Taking the ERA-interim reanalysis dataset (Simmons et al. 2006) as a set of initial conditions, tendencies generated by the primitive equations are used to diagnose the implied forcing of the observed mean annual cycle in each of the model's prognostic variables. These forcing functions are then separated into contributions from different timescales and from the interactions between timescales.

The second goal of this paper is to use these forcing terms to drive a dynamical model with an annual cycle. The diagnostics presented in the first part of the paper thus serve as an empirically derived cyclic forcing for the primitive equation model. The resulting simple GCM is called DREAM (Dynamical Research Empirical Atmospheric Model). It is an extension of a model that has been used for various climate studies using a range of forcing prescriptions (see for example, Hall 2000; Leroux et al. 2011; Hall et al. 2013). One limitation of the model until now has been that time-independent forcing was imposed, so only perpetual season integrations could be made. Here we extend the method to include a forced annual cycle. The resulting model simulation will be compared with the reanalysis. Comparisons will also be made with perpetual season integrations using the same model with constant seasonal forcing.

In Sect. 2, the theory is presented for deriving source terms from data using a model. A budget is defined for the forcing of the annual cycle, with contributions from the observed mean flow, the observed annual cycle and from their interactions with other timescales. Details of the dynamical model and the dataset are then given in Sect. 3. The annual cycle forcing budget for momentum, temperature and humidity is presented in Sect. 4. In Sect. 5 results from long integrations of the simple GCM are presented and compared with the reanalysis. All these results are discussed further in Sect. 6.

2 Forcing of the annual cycle

2.1 Diagnosis of forcing terms

The approach we adopt is to take a primitive equation model that contains only advective dynamics and simple dissipation, and initialise it from a series of observed states taken from a reanalysis dataset. This approach has been used several times to obtain the forcing needed for perpetual-season integrations of simple dynamical models (see for example Roads 1987; Marshall and Molteni 1993; Lin and Derome 1996; D'Andrea and Vautard 2000; Hall 2000; Sardeshmukh and Sura 2007). Similar methods have also been used to diagnose and correct systematic errors in GCMs (Klinker and Sardeshmukh 1992; Schubert and Chang 1996; Del-Sole and Hou 1999; Danforth et al. 2007). Here we extend the original empirical forcing method to the annual cycle. The procedure is to calculate a source term for the model's prognostic variables that will neutralise the initial systematic errors, chiefly associated with the model's lack of representation of physical processes.

Consider the generic development equation,

$$\frac{d\mathbf{\Phi}_i}{dt} + (\mathcal{A} + \mathcal{D})\mathbf{\Phi}_i = \mathbf{f}(t), \tag{1}$$

where $\mathbf{\Phi}$ is a vector representing all prognostic variables, $\mathcal{A}$ is a quadratic operator which represents advection and $\mathcal{D}$ is a linear operator which represents damping and dissipation. The forcing $\mathbf{f}$ is unknown and the object of this exercise is to diagnose it from an observed sequence of atmospheric states $\mathbf{\Phi}_i$ using a model that can provide $\mathcal{A}$ and $\mathcal{D}$. A further objective is to break down this forcing into contributions

to the time mean and the annual cycle arising from interactions between the time mean, the annual cycle and the transients. For the purposes of this article the "transients" are all time variations not represented by the annual cycle, and the annual cycle is the average annually repeating component of the variability (details of how it is calculated will be given in the next section). By construction, both transient and cycle components have zero long term mean.

We thus break down the variables into three components: climatological annual mean, mean annual cycle and transients: denoted by bar, tilde and prime respectively (note that here "transients" encompasses all variability other than the mean annual cycle, including interannual variability).

$$\mathbf{\Phi} = \overline{\mathbf{\Phi}} + \widetilde{\mathbf{\Phi}} + \mathbf{\Phi}', \quad \mathbf{f} = \overline{\mathbf{f}} + \widetilde{\mathbf{f}} + \mathbf{f}'.$$

Our interest is restricted to finding the time-mean and annual cycle of the forcing. This can be written down from (1) as

$$\overline{\mathbf{f}} + \widetilde{\mathbf{f}} = \frac{d\widetilde{\mathbf{\Phi}}}{dt} + (\overline{\mathcal{A}} + \widetilde{\mathcal{A}})(\overline{\mathbf{\Phi}} + \widetilde{\mathbf{\Phi}} + \mathbf{\Phi}') + \mathcal{D}(\overline{\mathbf{\Phi}} + \widetilde{\mathbf{\Phi}}), \tag{2}$$

where overbar or tilde applied to $\mathcal{A}$ means that the associated time filtering operation is applied after the action of $\mathcal{A}$ on $\mathbf{\Phi}$. This quadratic term in (2) can be expanded into eighteen terms: nine for the time mean and nine for the annual cycle. These terms generally represent fluxes, and most of them describe interactions between timescales. For example, they could be associated with the flux of temporal temperature variations by the time-mean flow, or the flux of the time-mean temperature by temporal variations in the flow.

To retain a tractable general problem for a numerical model, and to keep the quantity of information manageable, we gather these terms according to the interactions between timescales M (mean) C (annual cycle) and T (transients). The budget for a cyclic forcing with non-zero time mean can thus be written as

$$\overline{\mathbf{f}} + \widetilde{\mathbf{f}} = \text{TEND} + \text{MM} + \text{MC} + \text{CC} + \text{CT} + \text{TT}\,. \tag{3}$$

Each of these terms contributes either to $\overline{\mathbf{f}}$ or $\widetilde{\mathbf{f}}$ or both. They are derived from a set of experiments in which the unforced dynamical model $(\mathcal{A} + \mathcal{D})$ is integrated for one time step from a long sequence of initial conditions $\mathbf{\Phi}_i$. Carefully prepared sets of one-time step integrations are averaged together to deliver all the components of the forcing budget expressed in (3). Details of the method and a complete definition of the terms are given in the appendix. Note that MM has no annual cycle, but TEND and MC are purely cyclic with zero time mean. The remaining three terms CC, CT and TT have both time mean and annual cycle. Taken together these three terms represent the negative of what is normally considered the "transient eddy forcing".

2.2 Driving a simple GCM

The forcing $\overline{\mathbf{f}} + \widetilde{\mathbf{f}}$ is deduced from data by integrating the unforced model for one time step from the set of initial conditions $\mathbf{\Phi}_i$ (see Appendix). It can then be used to drive the model by adding it to the right hand side of the model equations and integrating from any initial condition through several annual cycles. So if we refer to model state vector as $\mathbf{\Psi}$ (in the same basis as $\mathbf{\Phi}$)

$$\frac{d\mathbf{\Psi}}{dt} + (\mathcal{A} + \mathcal{D})\mathbf{\Psi} = \overline{\mathbf{f}} + \widetilde{\mathbf{f}}. \tag{4}$$

This is the defining method for the DREAM model. The results can be compared with observations in the same way as one would validate a fully specified GCM. In fact such a model simulation can be directly compared with the same reanalysis data that was used to deduce the forcing in the first place. There is no guarantee that the simulation $\mathbf{\Psi}$ will be close to this reanalysis $\mathbf{\Phi}$. Although the total forcing budget will be identical, a model forced in this way is free to find its own balance of terms on the right hand side of (2). Combining the time means of (1) and (4) leads to the following constraint for the model simulation $\mathbf{\Psi}$

$$\overline{\mathcal{A}}(\overline{\mathbf{\Psi}} + \widetilde{\mathbf{\Psi}} + \mathbf{\Psi}') + \mathcal{D}(\overline{\mathbf{\Psi}}) = \overline{\mathcal{A}}(\overline{\mathbf{\Phi}} + \widetilde{\mathbf{\Phi}} + \mathbf{\Phi}') + \mathcal{D}(\overline{\mathbf{\Phi}}) = \overline{\mathbf{f}}. \tag{5}$$

In general the balance of terms in (5) will not be the same for $\mathbf{\Psi}$ and $\mathbf{\Phi}$. Indeed one would not expect it to be, as the model contains no interaction between transients and physical processes. Consequently $\overline{\mathbf{\Psi}} \neq \overline{\mathbf{\Phi}}$ and there will be systematic errors in both model climatology and model transient fluxes, as with any GCM. However, to the extent that the model contains an accurate representation of the advective dynamics $\mathcal{A}$, and a reasonable specification for $\mathcal{D}$, we expect the model climatology $\overline{\mathbf{\Psi}}$ to be fairly realistic.

The model can also be forced with the constant $\overline{\mathbf{f}}$. This results in a perpetual integration. $\overline{\mathbf{f}}$ as defined above is the annual mean forcing, but it can also be calculated from a subset of $\mathbf{\Phi}$, taken from just one season. This is how perpetual summer and winter simulations have been done in the studies cited above. In Sect. 5 comparisons will be made between cyclic and perpetual simulations.

The empirical approach to forcing a simple model outlined above can be compared with the widespread practice of restoration forcing, in which a dynamical core is typically forced on a timescale τ by the difference between the model state and a restoration state $\mathbf{\Phi}^*$. This is usually a zonally uniform temperature distribution that is deemed to represent radiative convective equilibrium (see Held and Suarez 1994).

$$\frac{d\mathbf{\Psi}}{dt} = \frac{(\mathbf{\Phi}^* - \mathbf{\Psi})}{\tau}.$$

Unless a free solution exists, there will be development and a statistical balance between forcing, dissipation and dynamical fluxes will ensue, as with our empirical forcing. The difference between our data-driven approach and this restoration forcing is that instead of specifying an unknown equilibrium state and a time scale, we specify the model dissipation independently, and deduce the forcing objectively from data. If $D(\mathbf{\Phi}) = \mathsf{D}\mathbf{\Phi}$ and D is linear and diagonal, i.e. all the dissipation is local, then the two methods are mathematically identical, with

$$\mathbf{\Phi}^* = \frac{\bar{\mathbf{f}}}{\mathsf{D} \cdot \mathbf{1}}.$$

In fact the DREAM model has linear vertical and horizontal diffusion and variable land-sea drag so it would not be straightforward to find an equivalent of $\mathbf{\Phi}^*$, and arguably of limited interest.

3 Model and data

The dynamical model used for DREAM was originally developed by Hoskins and Simmons (1975) and was first adapted for the empirical forcing technique by Hall (2000). It has since been used in a number of configurations to study for example the atmospheric response to El Nino (Hall and Derome 2000; Lin et al. 2007), African easterly waves (Hall et al. 2006; Thorncroft et al. 2008; Leroux and Hall 2009; Leroux et al. 2011) and tropical-extratropical interactions (Hall et al. 2013). Apart from adding an annual cycle to the forcing, the latest incarnation has a number of changes including increased resolution, a specific humidity variable and some modifications to the damping and diffusion.

The horizontal resolution is T42 with a semi-implicit 22.5-min time step to integrate the primitive equations expressed in terms of vorticity, divergence, temperature and log(surface pressure). Specific humidity is included as a passive tracer, with empirically derived sources and sinks. Since the model version used in this study has no representation of saturation, condensation and the associated diabatic heating, there is no link between specific humidity and the thermodynamic equation and thus no interaction with the dynamics. Orography is not represented explicitly in the model but its mean effect is implicitly included in the empirical forcing described above. The surface pressure used in the model is therefore calculated by integrating the barometric equation from 1000 hPa height to zero using the 1000 hPa temperature. Referenced to this pressure, the model has 15 sigma levels in the vertical that are designed to match the standard pressure levels of the reanalysis dataset as closely as possible. The model levels are $\sigma \times 1000 = 37.5$, 100, 150, 200, 250, 312.5, 400, 500, 600, 700, 791.67, 850, 883.33, 925, 975.

Horizontal dissipation takes the form of a scale selective 12-h ∇^6 diffusion applied to vorticity, divergence, temperature and specific humidity. Linear vertical diffusion between adjacent levels is also applied to the same variables, with a strength that decreases linearly from the surface to $\sigma = 0.8$ and is constant in the free atmosphere above. The average strength of the low-level vertical diffusion corresponds to a timescale of 16 h. In the free atmosphere the timescale is 20 days. The value at the lowest level is doubled over land for momentum. In addition a linear in-situ damping is applied to temperature with a timescale of 12 days independent of height. This can be identified with radiative cooling and may be compared with the restoration approach discussed in Sect. 2.

In this diagnostic study we use the ERA-interim reanalysis dataset of 4-times daily data over the 38-year period 1979–2016, for a total of 55520 time records. These data are spectrally analysed at T42 and linearly interpolated in the vertical onto the model sigma levels. We take the earth's orbital period to be 365.25 days, which corresponds to 1461 time records. An average of 38 such orbital periods is made (using all but the last two of the time records in the dataset). Our mean annual cycle is then produced by applying a 41-point (10-day) cyclic running mean to this average, to remove sub-seasonal variability associated with sampling a finite time series.

4 The forcing terms

The forcing $\bar{\mathbf{f}} + \widetilde{\mathbf{f}}$ is an annual cycle of source terms for model variables which represents processes and boundary fluxes that are not present explicitly in the model. These are the sources and sinks of momentum, temperature and humidity required to maintain the equilibrium expressed in (2). They are broken down in Eq. (3) into components associated with the mean flow, mean annual cycle and transients and these components will be examined in this section. Contributions to the mean forcing and its annual cycle can be expressed separately as

$$\bar{\mathbf{f}} = \mathrm{MM} + \overline{\mathrm{CC}} + \overline{\mathrm{CT}} + \overline{\mathrm{TT}}$$
$$\widetilde{\mathbf{f}} = \mathrm{TEND} + \mathrm{MC} + \widetilde{\mathrm{CC}} + \widetilde{\mathrm{CT}} + \widetilde{\mathrm{TT}}.$$

First we will consider the annual mean total forcing. Zonal mean sections of $\bar{\mathbf{f}}$ are shown in Fig. 1 for zonal wind, temperature and specific humidity. It appears that the principal budget residual for momentum forcing is a drag that opposes low-level zonal wind, probably mostly associated with the absence of explicit orography in the model. Low-level

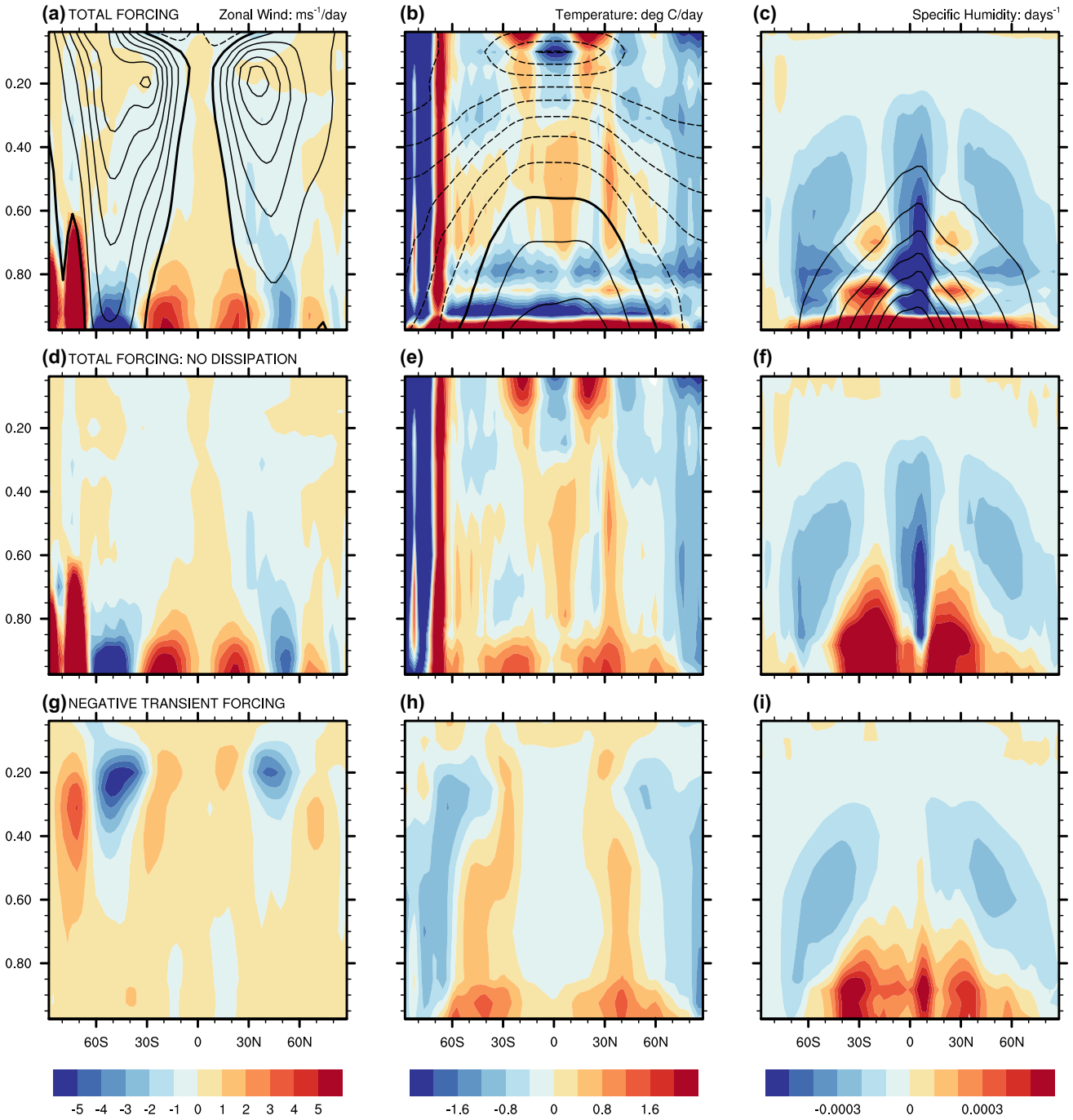

Fig. 1 Time-mean annual mean zonal mean for the forcing $\bar{\mathbf{f}}$ required to correct one-timestep systematic errors in the full primitive equation model (top row: **a**–**c**) and in the same model with no dissipation (middle row **d**–**f**). The bottom row (**g**–**i**) shows the transient component: i.e. the total forcing $\bar{\mathbf{f}}$ minus the mean flow component MM (see text). Left column (**a**, **d**, **g**) zonal wind: m.s^{-1}/day. Middle column (**b**, **e**, **h**) temperature: K/day. Right column (**c**, **f**, **i**) specific humidity: days^{-1}. Contours in the top row show mean fields for reference: intervals for **a** 5 m s^{-1}; **b** 10 K; **c** 10^{-4}. Zero contour bold, negative dashed

mean forcing of temperature and humidity is dominated by a source at the surface and a sink in the upper boundary layer that essentially redresses the low-level modification of mean quantities by the model's vertical diffusion scheme. This could be identified physically with surface fluxes and radiation, but it is clearly entirely conditioned by the choices made for model dissipation D. To express the forcing budget associated with dynamics alone, a second set of calculations was made with all model dissipation switched off ($\mathsf{D} = 0$), shown in the second row of Fig. 1. The low-level dipoles

disappear and what remains are sources and sinks of heat and moisture due to boundary fluxes, evaporation and condensation and their diabatic effects. This is particularly evident in the tropical mid-troposphere and upper atmosphere associated with the mean divergent circulation. Sources and sinks of humidity are clearly associated with the mean Hadley circulation. The diagnosed forcing supplies humidity in the subtropics, which is then advected equatorwards and lifted to the mid-troposphere where negative values of forcing denote condensation. Poleward and upward transfer of moisture in the storm tracks is also reflected by two further condensation maxima in the mid-latitudes.

The bottom row in Fig. 1 shows the total transient covariance component of $\overline{\mathbf{f}}$: $\overline{\mathrm{CC}} + \overline{\mathrm{CT}} + \overline{\mathrm{TT}}$. This is the negative of what is commonly referred to as the "transient eddy forcing". Transient fluxes are explicit in the dynamics of the model and present in the reanalysis, so this component of $\overline{\mathbf{f}}$ is the forcing that would be necessary to compensate for these fluxes. It often cancels with the mean component MM, as is clearly the case for the momentum forcing in the tropospheric jets, where negative values in Fig. 1g pick out regions of transient eddy acceleration of the westerlies. This is balanced by the action of the Coriolis force on the mean meridional circulation so the net forcing $\overline{\mathbf{f}}$ is small. Transient components of $\overline{\mathbf{f}}$ for temperature and humidity also pick out the action of the mid-latitude storm tracks but in this case the transient fluxes are to some extent balanced by real diabatic effects, so their signature is visible in the total forcing $\overline{\mathbf{f}}$.

Note that since the model diffusion is linear, it has no influence on the diagnosis of the transient components, and the bottom row of Fig. 1 is not affected by the inclusion of D in the calculation. Nevertheless, for the sake of clarity, all further diagnostics in this section are from the dissipation-free version of the model.

Apart from MM, all components of (3) have an annual cycle and this is shown in Figs. 2 and 3 for the zonal mean temperature. The top row of Fig. 2 shows the tendency component TEND for the four usual seasons based on calendar months. The solstice seasons DJF and JJA show very small tendencies and, compared to the total forcing, values also remain small in the equinox seasons. MAM shows northern hemisphere warming and southern hemisphere cooling and SON shows the opposite but note that all values are multiplied by ten in the figure. The CT term is even smaller, with values multiplied by 100 in the bottom row of Fig. 2. So as one might expect, covariance is negligible between the annual cycle of one dynamical component of a flux and predominantly much shorter timescale transients in the other component. There is, nevertheless, a very weak but systematic signature, in opposition to the upward transfer of heat in the seasonal storm track.

The other three terms that make up the annual cycle of temperature forcing: MC, CC and TT are shown in Fig. 3 with the same units as in Fig. 1. The term MC term can be understood as the forcing that would be required to balance a combination of the flux of annual mean temperature by the seasonal anomaly winds, and the flux of the seasonal

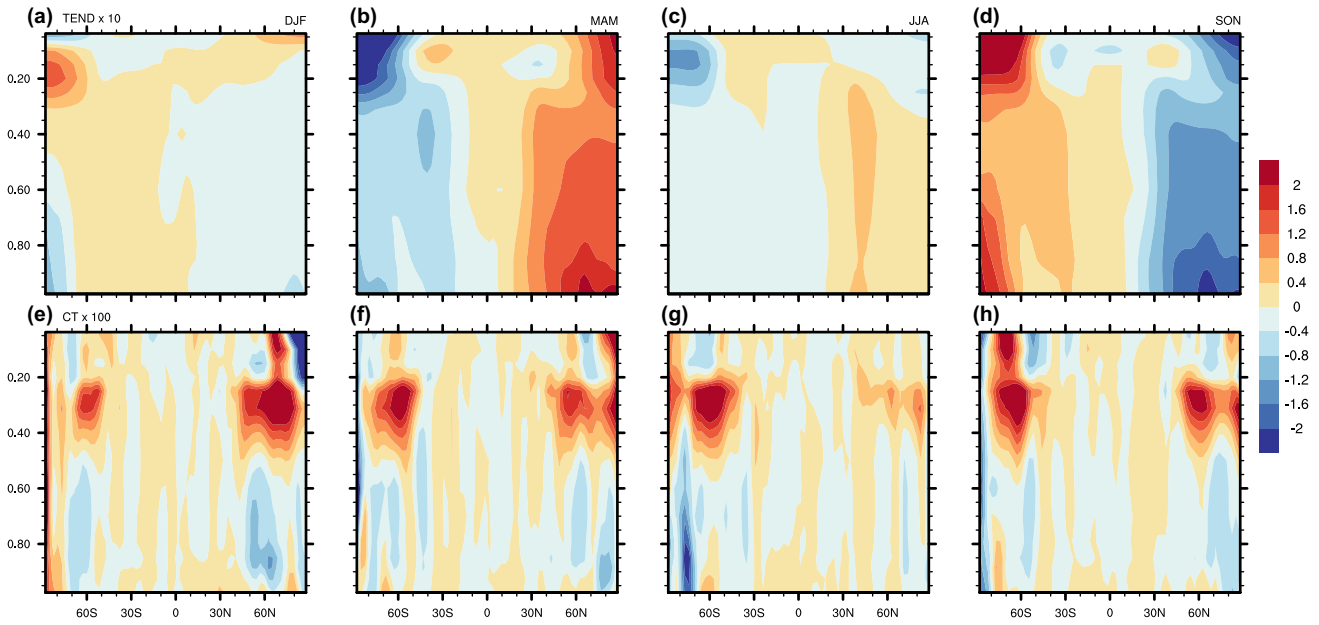

Fig. 2 Seasonal values for the zonal mean forcing of temperature in K/day. Top row (**a**–**d**) tendency component TEND multiplied by 10; bottom row (**e**–**h**) annual cycle-transient interaction term CT multiplied by 100. Columns left to right are DJF (**a**, **e**), MAM (**b**, **f**), JJA (**c**, **g**) and SON (**d**, **h**)

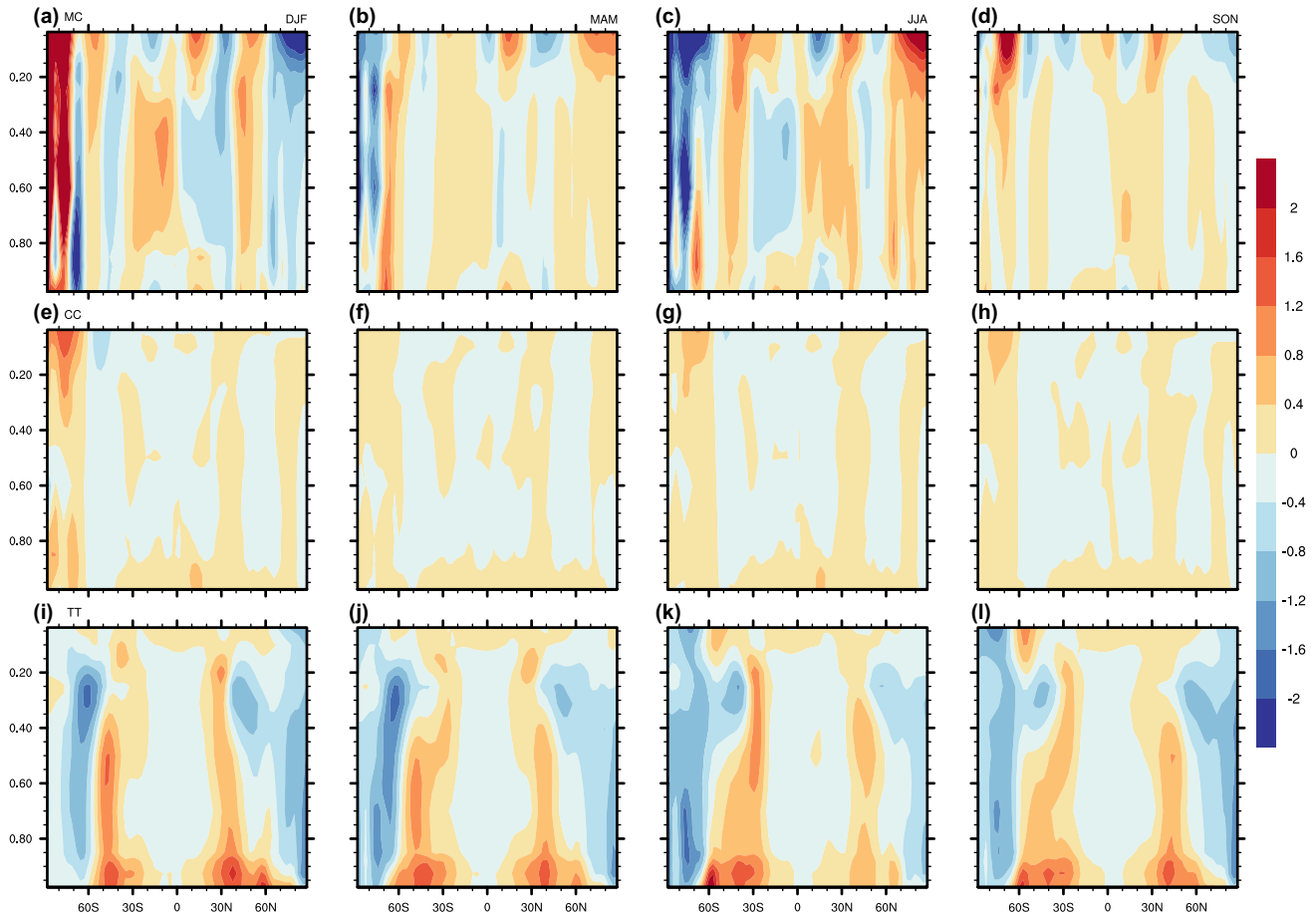

Fig. 3 Seasonal values for the zonal mean forcing of temperature in K/day. Top row (**a**–**d**) mean-cycle interaction term MC; middle row (**e**–**h**) cycle-cycle interaction term CC; bottom row (**i**–**l**) transient-transient interaction term TT. Columns left to right are DJF (**a**, **e**, **i**), MAM (**b**, **f**, **j**), JJA (**c**, **g**, **k**) and SON (**d**, **h**, **l**)

anomaly of temperature by the annual mean winds. Our diagnostic method (see Appendix) can only give the sum of these two effects and can't distinguish between them. The MC component appears to be approximately equal and opposite in DJF and JJA and weak in the equinox seasons (remember that the annual mean of MC is zero). Transient covariances are represented by the CC and TT components of **f** and are shown on the second and third rows of Fig. 3 respectively. Annual cycle covariances, i.e. the fluxes of seasonal anomaly temperature by seasonal anomaly winds (CC) are relatively weak. Covariances outside the annual cycle (TT) display the familiar signature of the seasonally varying storm tracks.

Figure 4 shows the same set of plots as Fig. 3 for specific humidity forcing. The MC component picks out the seasonal reversal of the Hadley cell. Negative values of forcing denote removal of humidity by precipitation and positive values denote an evaporative source. In this case the transient term TT shows a weak annual cycle and of course from this diagnostic alone we cannot identify the associated time scale without further time filtering. Interestingly the CC term is not small everywhere for humidity. There is a region at low levels just north of the equator where it is substantial, and positive all year round. This is examined further in Figs. 5 and 6 which show horizontal distributions for $\sigma = 0.85$. The annual mean component MM (Fig. 5) depicts extensive evaporative source regions over the eastern subtropical oceans and condensation in the narrow maritime ITCZ and SPCZ rain bands, with more dispersed rainfall over the continents. Midlatitude synoptic systems manifest in the storm track regions in the TT term, mostly in terms of an evaporative source at this level, with condensation occurring higher and further north.

The CC term presents a dipole over the African northern tropics. There is a source region over land along the Guinea coast and eastwards into the continent, and a parallel strip of condensation in the Sahel region to the north. The seasonal dependence of this phenomenon is laid out in Fig. 6, which shows a marked contrast between the MC and CC components of the forcing. As seen in Fig. 4 the MC term shows

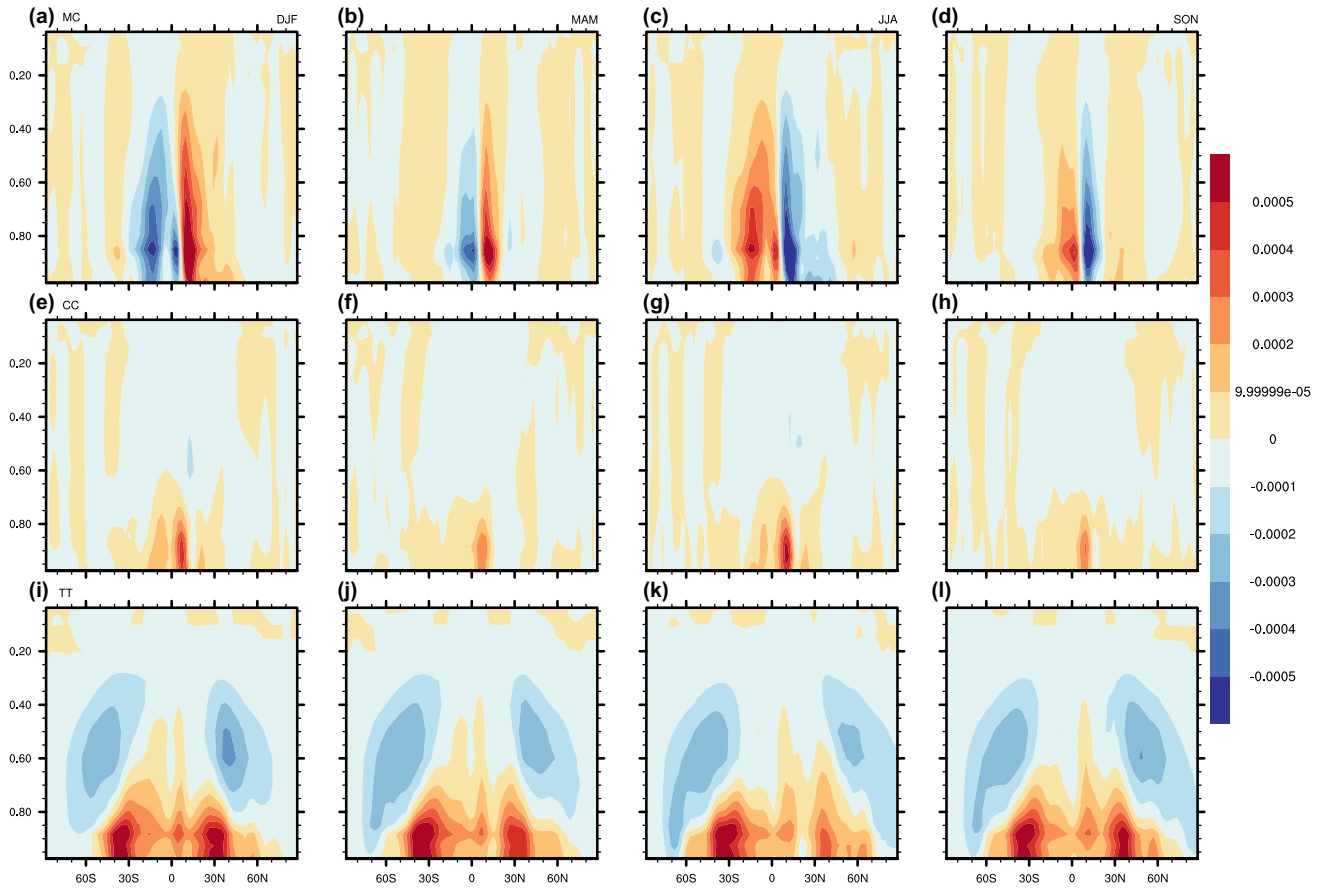

Fig. 4 As Fig. 3 but for the zonal mean forcing of specific humidity in days^{-1}

a seasonal shift in tropical hydrology associated with the reversal of the Hadley cell and the West African monsoon. The change in sign between DJF and JJA is clearest over the tropical Atlantic, but it is also evident over the Sahel. There is no such sign change in the CC term. The distribution over West Africa, where the signal is strongest, is remarkably similar in DJF and JJA.

So during DJF there is cancellation between MC and CC and during JJA they reinforce. The result is an enhanced northward migration of rainfall during boreal summer as seen in the bottom row of Fig. 6 which shows the forcing deduced from all advective terms (i.e. everything except TEND in (3)).

The associated fluxes of specific humidity q can be characterised as follows. The annual mean low-level flow converges at a humidity maximum just off the Guinea coast (MM). In summer, onshore flow displaces this q maximum onto the continent (MC). Increased continental moisture is then redistributed with greater convergence to the north and weaker convergence to the south (CC). The monsoon thus displaces into the Sahel. In the winter there is divergence over the continent and strong convergence over the ocean so the q maximum is displaced offshore (MC). Since the divergence increases northwards and the anomaly in q is negative, the dipole in CC retains the same sign, thus cancelling MC and ensuring there is minimal moisture supply to the continent. The associated annual cycles of circulation and humidity have been analysed by Thorncroft et al. (2011) (see their Fig. 6). The two-stage monsoon onset described above is consistent with these observed seasonal anomalies and has recently been modelled by Peyrillé et al. (2016) in an idealised two-dimensional framework. On the eastern side of the continent the seasonality of rainfall has similarly been shown by Yang et al. (2015) to be related to covariance between divergence and static stability.

5 GCM integrations

The mean plus annual cycle forcing $\bar{\mathbf{f}} + \tilde{\mathbf{f}}$ is now used to drive a long integration of the DREAM model. The integration is the same length as the ERAi dataset: 38 years from 1979 to 2016, and it is initialised with the ERAi state from 0Z 1/1/1979. The diagnostics presented here are taken from the period 1 March 1979 to 30 November 2016, to match full seasons from the dataset. This also provides ample spinup

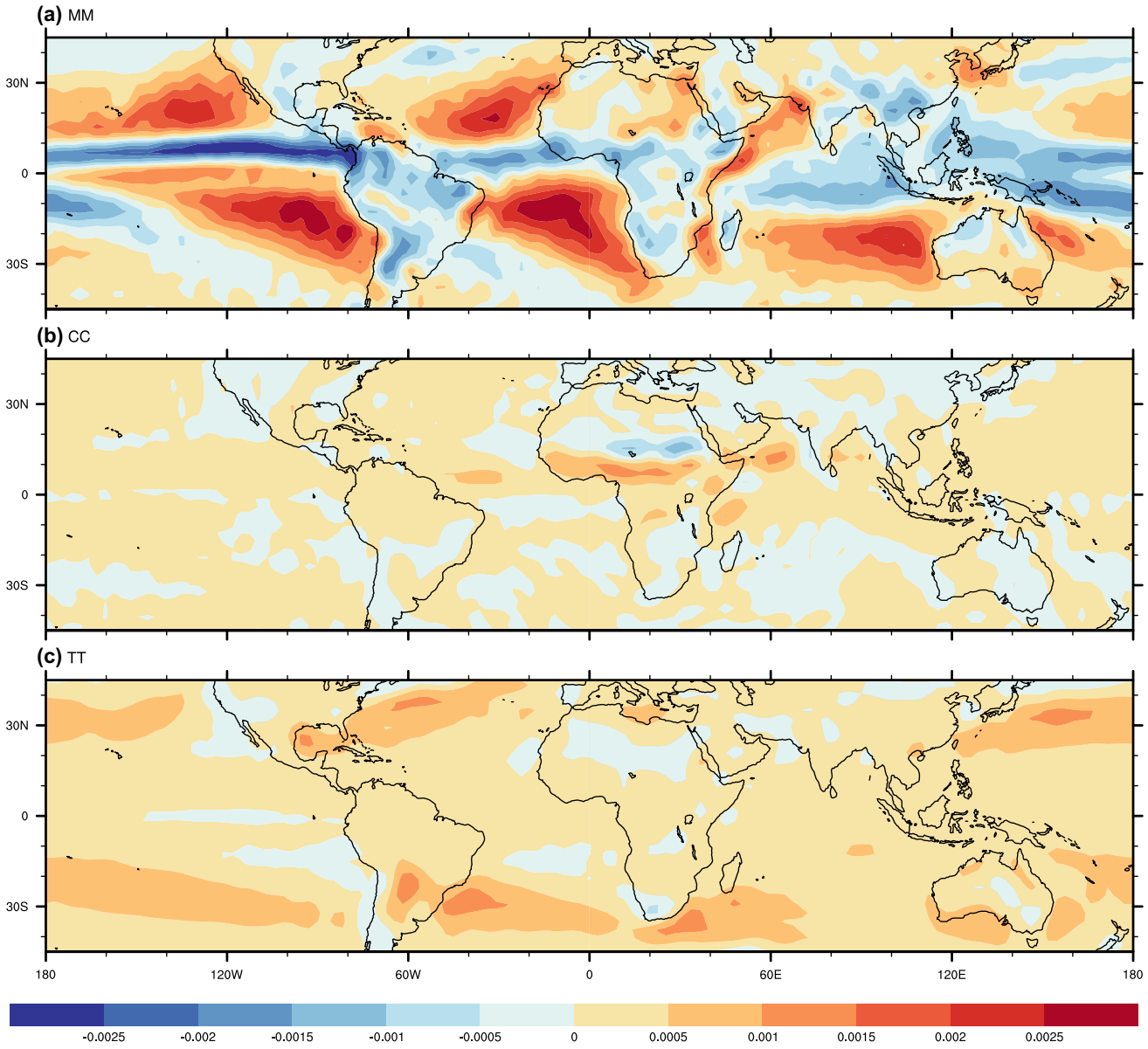

Fig. 5 Tropical and subtropical forcing of specific humidity in days^{-1} on the $\sigma = 0.85$ level for **a** the mean flow component MM; **b** the cycle-cycle interaction term CC and **c** the transient-transient interaction term TT

time for the model to ensure that the results are independent of the initial condition. Four perpetual runs were also carried out using a time-independent forcing $\bar{\mathbf{f}}$ calculated from subsets of the dates pertaining to the four seasons. These runs were initialised from the first time record occurring in in each respective season in 1979. The first 30 days was discarded from each run and results are presented for the following 3420 (= 38×90) days.

The seasonal mean zonal wind at $\sigma = 0.25$ from the five model runs is compared with the reanalysis in Fig. 7 for the four seasons. The winter (DJF) simulation with annual cycle forcing (Fig. 7b) compares well with the reanalysis (Fig. 7a), especially in the northern hemisphere. The southern hemisphere jet is slightly too weak and fragmented in longitude. It appears to be split between subtropical and mid-latitudes. The perpetual run (Fig. 7c) is very similar in the winter. The next row shows spring (MAM) and the model is again very close to the reanalysis. The observed splitting of the southern hemisphere jet is reproduced, if somewhat exaggerated. This time the perpetual run is slightly different and the subtropical southern hemisphere flow is more dominant, and in general the peak westerlies are too strong. In summer (JJA) both cycle and perpetual runs share the main systematic error of a southern hemisphere subtropical jet that is too

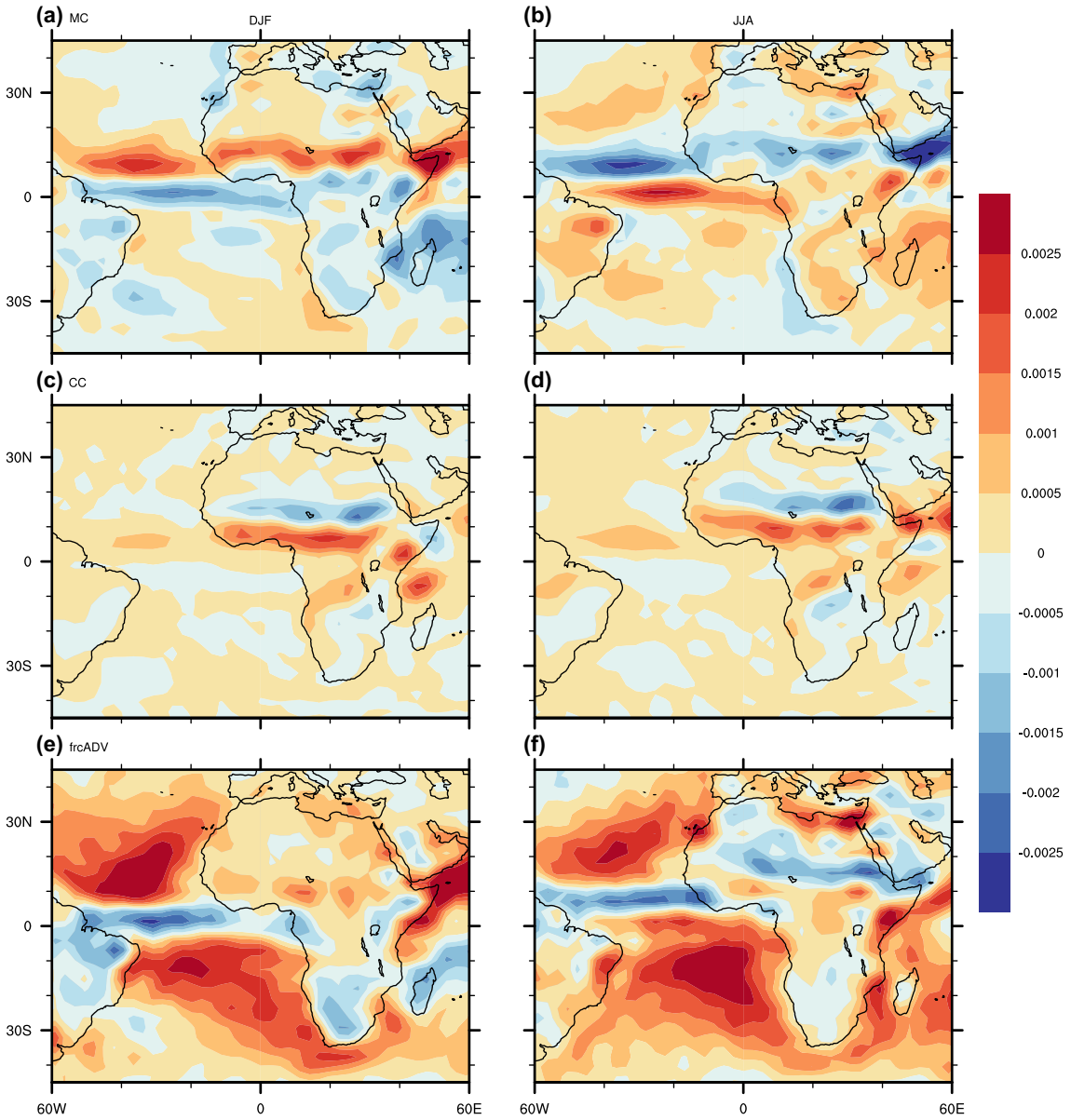

Fig. 6 Seasonal values of specific humidity forcing in days^{-1} on the $\sigma = 0.85$ level over Africa and the tropical and subtropical Atlantic. Top row (**a**, **b**) mean-cycle term MC; middle row (**c**, **d**) cycle-cycle component CC. The bottom row (**e**, **f**) shows the total advective contribution to the annual cycle of $\bar{\mathbf{f}}$, i.e. $\bar{\mathbf{f}} + \tilde{\mathbf{f}}$–TEND. Left (**a**, **c**, **e**) DJF; right (**b**, **d**, **f**) JJA

intense, although again slightly worse in the perpetual case. This error persists into the autumn (SON) as the westerlies return quite realistically to the northern hemisphere.

Transient meridional fluxes of temperature at $\sigma = 0.85$ are shown in Fig. 8. Unfiltered fluxes are shown to ease comparison with the forcing terms shown in the previous section. The storm tracks are well located in the northern hemisphere, but systematically too far south in the southern hemisphere winter (JJA and SON). The other main systematic error is that the storm tracks are too weak (although well located) in the summer hemisphere. This is particularly noticeable for the southern storm tracks in DJF. In all cases for this diagnostic there is very little discernible difference between the seasonal means from the cycle run and the corresponding perpetual runs.

Transient fluxes at upper levels reveal further systematic errors in the southern hemisphere. Figure 9 shows the momentum flux at $\sigma = 0.25$. In the northern hemisphere winter the model produces transient fluxes of realistic magnitude and these fluxes are convergent in the jet exit regions, indicating some degree of realism in the transient contribution to the momentum budget. The northern hemisphere annual cycle appears satisfactory but in the southern hemisphere the fluxes are weak, especially in the

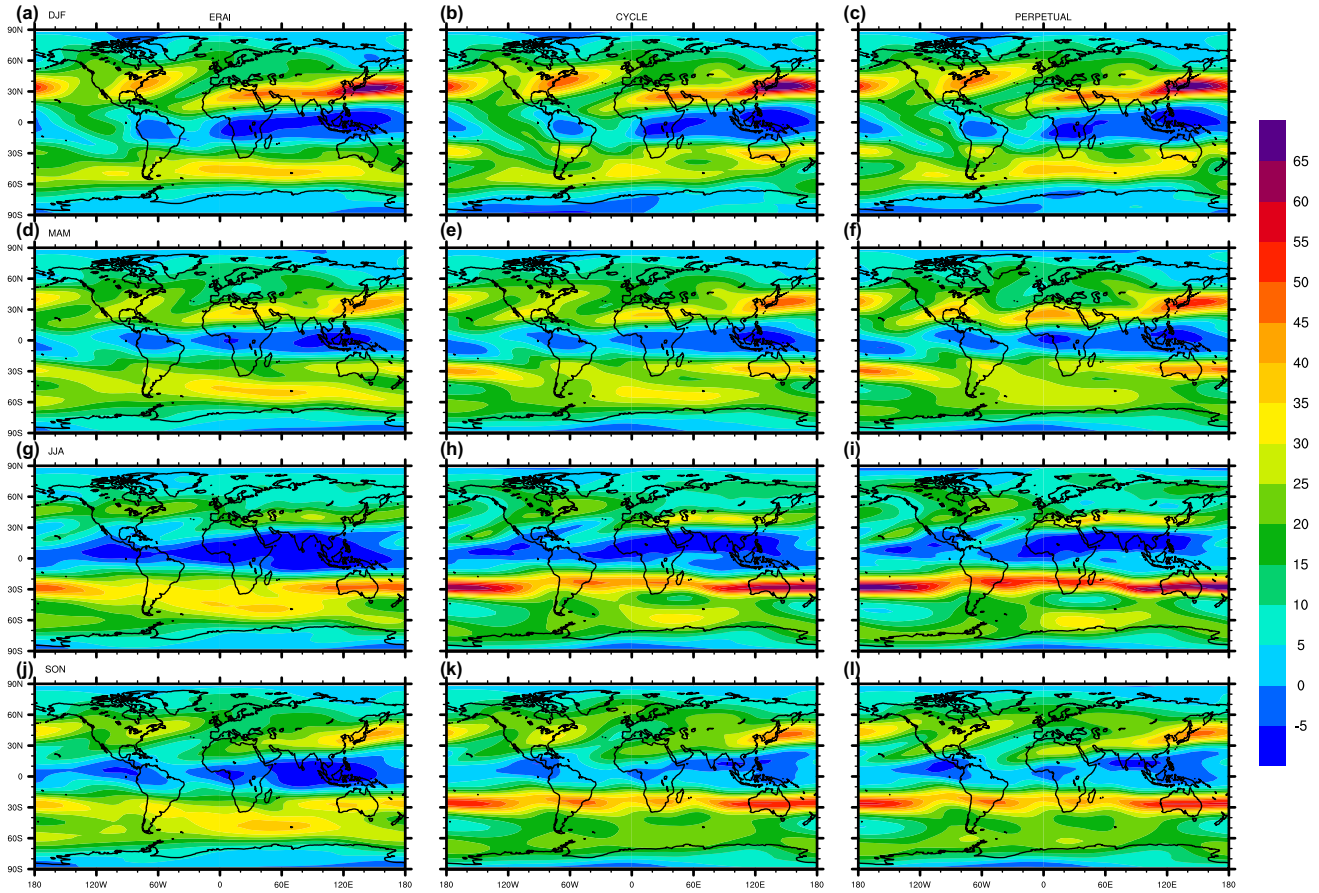

Fig. 7 Time-mean zonal wind u in m s^{-1} on the $\sigma = 0.25$ level. Left column (**a**, **d**, **g**, **j**) shows seasonal means from the ERA-interim reanalysis. Middle column (**b**, **e**, **h**, **k**) shows seasonal means from the annual-cycle DREAM run. Right column (**c**, **f**, **i**, **l**) shows time-means from perpetual DREAM runs. Rows top to bottom are the seasons DJF (**a**–**c**), MAM (**d**–**f**), JJA (**g**–**i**) and SON (**j**–**l**)

austral winter. The empirical forcing anticipates strong zonal mean momentum fluxes in the south (Fig. 1g) but the model does not deliver, even though the southern hemisphere jet is strong, and sometimes too strong in the subtropics. The solution adopted by the model clearly has a different transient-mean flow balance (Eq. 5) associated with a weak meridional circulation, weak transients and a strong displaced jet. Again, the differences between cycle and perpetual runs are very small.

In summary the model provides a dynamical simulation that is mostly realistic, with a faithful representation of zonal flow and stationary waves, reasonable low level transient fluxes in the storm tracks and an annual cycle that is in phase with the observations. The main exception to this is the upper level transient momentum flux in the southern hemisphere and the associated dynamical balance with the jet. In most respects, perpetual seasonal runs give a very close facsimile of the cycle run, with a slight tendency to aggravate the systematic errors.

6 Discussion

In this study the ERA-interim reanalysis has been interrogated with a dynamical model to provide a general budget residual forcing term which can in turn be used to drive the model, allowing it to serve as a simple GCM. The resulting forcing can be associated with physical processes and boundary conditions. It has been broken down into a number of contributions from different timescale interactions.

Our main focus has been the annual cycle so timescale contributions to the interaction terms have been split into an annual mean M, a mean annual cycle C and other timescales T. Unsurprisingly, T includes a large contribution from the extratropical storm tracks, and the covariance term CT is generally negligible. However, CC and TT both contribute to the annual cycle and separating these contributions from terms that are linear in the annual cycle has proved quite revealing.

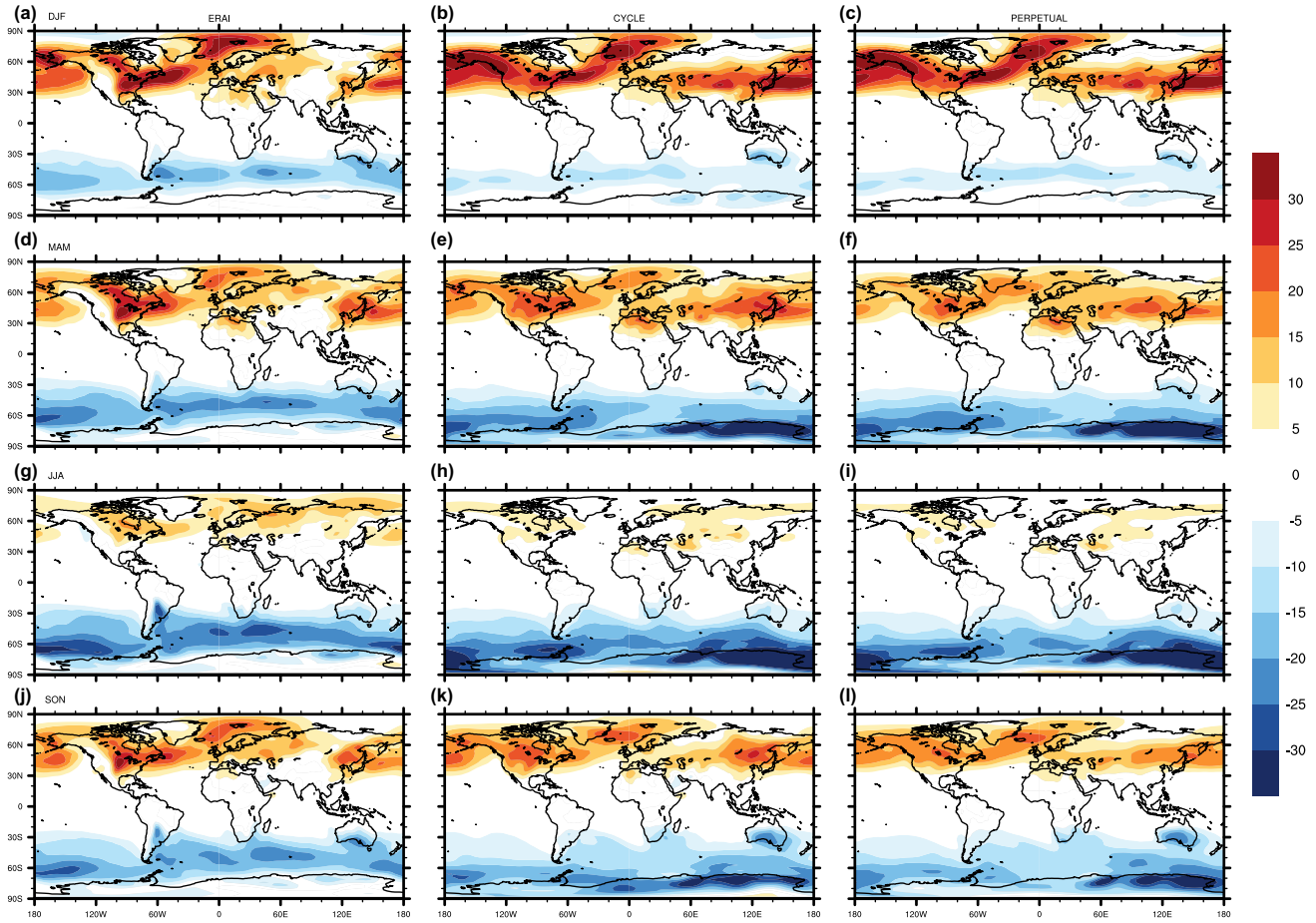

Fig. 8 As Fig. 7 but for the unfiltered transient meridional temperature flux $\overline{v'T'}$ on the $\sigma = 0.85$ level in K m s^{-1}

One unexpected result that emerged from this data analysis is a novel account of the moisture supply to the West African monsoon. Whereas other monsoons may be characterised chiefly in terms of changes in the low-level wind, the West African monsoon, and in particular its extension into the Sahel, depends not only on the separate contributions of seasonal variations in wind direction and humidity, but also on the covariance of their seasonal anomalies. In the winter the convergence of humidity flux is confined near the coast but in the summer it moves north into the Sahel. This is partly explained by seasonal changes in the wind, but the effect is reinforced as the southerly wind also transports the seasonally increased coastal humidity. Unlike the mean-cycle term, the covariance component of the humidity budget does not change sign, so it amplifies the monsoon in the summer and cancels it in the winter. This characteristic emerges from the analysis quite strongly over West Africa compared to other monsoon regions.

When the dynamical model is pressed into service as a simple GCM, with or without an annual cycle, it generally delivers a level of realism that will allow it to serve as a useful tool in many applications. The main systematic error related to the momentum balance in the southern hemisphere is not new to this model, and has not been improved by the introduction of an annual cycle in the forcing. Increased resolution and the introduction of vertical diffusion have also had little impact. Hall (2000) tried an ad-hoc boost to the forcing of the temperature gradient with limited success. Another potential fix would be to reduce the surface drag over the southern ocean to boost the meridional circulation and thus modify the upper level momentum balance, but this would also be an ad-hoc solution. A more satisfying approach might involve the objective specification of spatial and temporal variations in $\mathcal{D}$, in a similar way to what is currently done for $\mathbf{f}$. But as well as being perhaps more difficult to justify physically, this would also be a far more complicated optimisation problem. It may be a fruitful avenue for future research.

The primary objective of extending the simple GCM beyond perpetual season integrations led us to consider a time-dependent forcing term that would balance seasonally evolving model systematic errors. This is why we focused

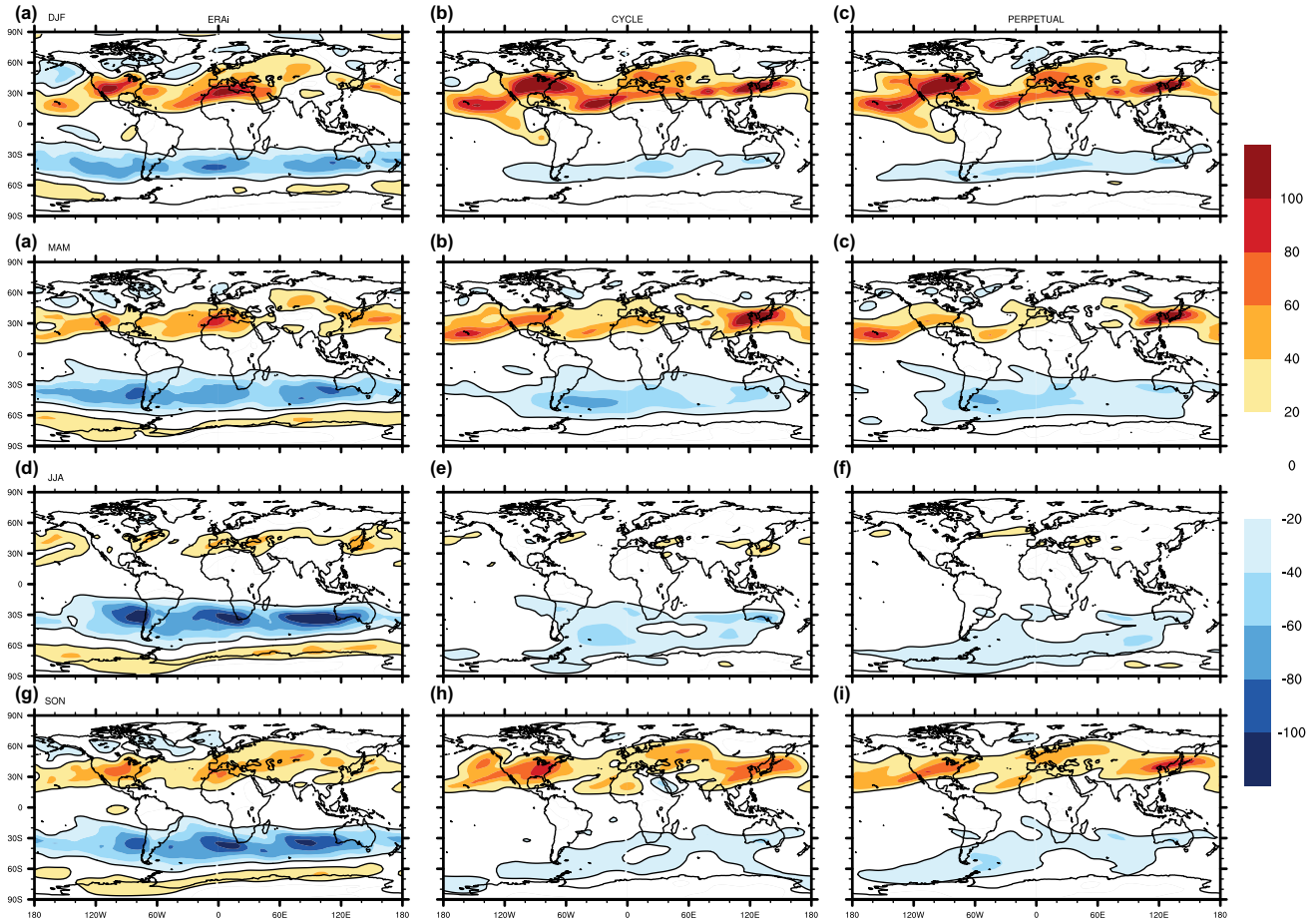

Fig. 9 As Fig. 8 but for the unfiltered transient momentum flux $\overline{u'v'}$ on the $\sigma = 0.25$ level in $m^2\ s^{-2}$. Contours have been added at $\pm$ 20 to improve readability

our budget analysis on the annual cycle. In fact, as expected, the tendency term associated with the annual cycle is small and consistent with this it has been demonstrated that perpetual seasonal runs with time-independent forcing mimic the seasonal means from the annual cycle run quite closely, even in the equinox seasons.

However, the cyclically-forced version of DREAM now permits further applications that were not possible in the perpetual configuration. It will be used for studies in which some time-dependent correspondence is needed between the model and observations. Of particular interest are cases where part of the solution is constrained by data (e.g. regional nudging), or where a time-evolving boundary condition is applied (e.g. a developing sea surface temperature anomaly). The facility to do perpetual runs with the same model, and with similar model climatology, is a further advantage.

Methodologically, the approach introduced in this paper, using the model to diagnose contributions from different timescale interactions, is not restricted to the annual cycle. Now that it has been tested in that context, there is ample scope for further applications. For example, interactions between high and low frequency transients could be diagnosed to study the generation, maintenance and impact of intraseasonal variations.

In the immediate future, the inclusion of an annual cycle in the DREAM model opens the door to many new types of experiment in which an idealised GCM can be compared with or constrained by data and can be used to complement investigations using fully specified GCMs.

Acknowledgements We thank the two anonymous reviewers for comments that led to some clarifications in the manuscript. The forcing budget calculations were carried out by N. Hall while visiting the Department of Atmospheric Sciences, University of Sao Paulo under FAPESP grant 08/58101-9. T. Ambrizzi received support from FAPESP Proc. No. 2017/09659-6.

Table 1 Terms in the forcing budget

Term	Definition	Contributes to	Description
TEND	$d\widetilde{\mathbf{\Phi}}/dt$	$\widetilde{\mathbf{f}}$	Tendency of annual cycle
MM	$\mathcal{Q}(\overline{\mathbf{\Phi}},\overline{\mathbf{\Phi}})+\mathcal{D}(\overline{\mathbf{\Phi}})$	$\overline{\mathbf{f}}$	Time-mean advection and dissipation
MC	$\mathcal{Q}(\overline{\mathbf{\Phi}},\widetilde{\mathbf{\Phi}})+\mathcal{Q}(\widetilde{\mathbf{\Phi}},\overline{\mathbf{\Phi}})+\mathcal{D}(\widetilde{\mathbf{\Phi}})$	$\widetilde{\mathbf{f}}$	Mean-cycle interaction
CC	$\mathcal{Q}(\widetilde{\mathbf{\Phi}},\widetilde{\mathbf{\Phi}})$	$\overline{\mathbf{f}}$ and $\widetilde{\mathbf{f}}$	Cycle–cycle interaction
CT	$\mathcal{Q}(\widetilde{\mathbf{\Phi}},\mathbf{\Phi}')+\mathcal{Q}(\mathbf{\Phi}',\widetilde{\mathbf{\Phi}})$	$\overline{\mathbf{f}}$ and $\widetilde{\mathbf{f}}$	Cycle-transient interaction
TT	$\mathcal{Q}(\mathbf{\Phi}',\mathbf{\Phi}')$	$\overline{\mathbf{f}}$ and $\widetilde{\mathbf{f}}$	Transient-transient interaction

Appendix: forcing budget definitions and calculations

It is convenient to adopt a more flexible notation for the expansion of Eq. (2). The operation of the dynamical model can be expressed as

$$(\mathcal{A}+\mathcal{D})(\mathbf{\Phi})=\mathcal{Q}(\mathbf{\Phi},\mathbf{\Phi})+\mathcal{D}(\mathbf{\Phi})=\Phi^{\dagger}\mathsf{Q}\mathbf{\Phi}+\mathsf{D}\mathbf{\Phi},$$

where $\Phi^{\dagger}$ is the diagonal matrix whose diagonal is formed from elements of the column vector $\mathbf{\Phi}$, and Q and D are real matrices. If $\mathbf{\Phi}$ is split into components $\mathbf{X}$ and $\mathbf{Y}$, the quadratic term $\mathcal{Q}(\mathbf{X},\mathbf{Y})=\mathsf{X}^{\dagger}\mathsf{Q}\mathbf{Y}$ is the column vector with elements $X_i(\sum_j Q_{ij}Y_j)$. Note that $\mathcal{Q}(\mathbf{X},\mathbf{X})=\mathcal{A}(\mathbf{X})$ and $\mathcal{Q}(\mathbf{X},\mathbf{Y})\neq\mathcal{Q}(\mathbf{Y},\mathbf{X})$.

In this notation the terms in the time mean-annual cycle forcing budget (3) can be written out individually and they are given in Table 1 along with a brief description and a reminder of which component of the forcing $\mathbf{f}$ they contribute to.

To find all these forcing terms the reanalysis dataset must be sampled in a variety of ways. The dataset $\mathbf{\Phi}$ consists of 4× daily data for 38 years, for a total of 55520 data records. The mean annual cycle $(\overline{\mathbf{\Phi}}+\widetilde{\mathbf{\Phi}})$ is a 365.25-day dataset consisting of 1461 data records. TEND is calculated directly from this dataset as the cyclic centred difference

$$\text{TEND}=\frac{\mathbf{\Phi}^{+}-\mathbf{\Phi}^{-}}{12hrs}$$

All the other terms are formed from one-timestep integrations of the unforced model.

$$\frac{d\mathbf{\Psi}}{dt}+(\mathcal{A}+\mathcal{D})\mathbf{\Psi}=0\ \ \rightarrow\ \ (\mathcal{A}+\mathcal{D})\mathbf{\Psi}=-\frac{d\mathbf{\Psi}}{dt}.$$

Values of this negative tendency taking various sets of initial conditions from the dataset $\mathbf{\Phi}_i$ are used to deduce the terms in (3).

Firstly, to find the sum of all the terms in (3) except TEND, the unforced model must be initialised using the entire dataset $\mathbf{\Phi}_i$. The mean and annual cycle from the resulting set of 55520 one-timestep forecasts, together with TEND, will furnish the forcing $\overline{\mathbf{f}}+\widetilde{\mathbf{f}}$. This is all that is needed to find a cyclic forcing for a simple GCM.

To break down the forcing into components we proceed as follows:

To find MM, a single integration is needed, with $\overline{\mathbf{\Phi}}$ as the initial condition. This gives $(\mathcal{A}+\mathcal{D})\overline{\mathbf{\Phi}}=$ MM.

To find the annual cycle contributions MC and CC we use the mean annual cycle $(\overline{\mathbf{\Phi}}+\widetilde{\mathbf{\Phi}})$ as a set of initial conditions. The negative one-timestep tendencies from these 1461 unforced integrations will deliver MM+MC+CC and since we know MM we can deduce MC+CC.

To separate MC from CC another experiment is required with a set of initial conditions $(\overline{\mathbf{\Phi}}+\alpha\widetilde{\mathbf{\Phi}})$. Since $\mathcal{A}$ is quadratic this will deliver MM $+2\alpha$ MC $+\alpha^2$ CC and algebraic elimination with the previous result will provide MC and CC. The value of α is arbitrary and tests confirm that varying α does not change the result.

To find the transient contributions CT and TT we use the entire dataset $(\overline{\mathbf{\Phi}}+\widetilde{\mathbf{\Phi}}+\mathbf{\Phi}')$ as a set of initial conditions as already discussed above. These 55520 unforced integrations will deliver MM + MC + CC + CT + TT and thence CT+TT. To separate CT from TT another set of initial conditions $(\overline{\mathbf{\Phi}}+\widetilde{\mathbf{\Phi}}+\alpha\mathbf{\Phi}')$ is used to get MM + MC + CC $+2\alpha$ CT $+\alpha^2$ TT. CT and TT are again deduced by algebraic elimination. Only the mean and annual cycle components of CT and TT are of interest in our budget for $\overline{\mathbf{f}}+\widetilde{\mathbf{f}}$.

In some of the results the damping and diffusion have been removed, but this is not done by algebraically separating $\mathcal{D}$ from $\mathcal{A}$. Instead the model is simply rerun with damping and diffusion switched off and the the same procedure is followed.

References

Biasutti M, Battisti DS, Sarachik E (2003) The annual cycle over the tropical atlantic, south america, and africa. J Clim 16(15):2491–2508

Chen YY, Jin FF (2017) Dynamical diagnostics of the sst annual cycle in the eastern equatorial pacific: part ii analysis of cmip5 simulations. Clim Dyn 49(11–12):3923–3936

D'Andrea F, Vautard R (2000) Reducing systematic errors by empirically correcting model errors. Tellus A Dyn Meteorol Oceanogr 52(1):21–41

Danforth CM, Kalnay E, Miyoshi T (2007) Estimating and correcting global weather model error. Mon Weather Rev 135(2):281–299
DelSole T, Hou AY (1999) Empirical correction of a dynamical model. part i: Fundamental issues. Mon Weather Rev 127(11):2533–2545
Fasullo JT, Trenberth KE (2008a) The annual cycle of the energy budget. part i: global mean and land-ocean exchanges. J Clim 21(10):2297–2312
Fasullo JT, Trenberth KE (2008b) The annual cycle of the energy budget. part ii: meridional structures and poleward transports. J Clim 21(10):2313–2325
Hall NMJ (2000) A simple GCM based on dry dynamics and constant forcing. J Atmos Sci 57:1557–1572
Hall NMJ, Derome J (2000) Transience, nonlinearity, and Eddy feedback in the remote response to El Niño. J Atmos Sci 57:3992–4007
Hall NMJ, Douville H, Li L (2013) Extratropical summertime response to tropical interannual variability in an idealized gcm. J Clim 26(18):7060–7079
Hall N, Kiladis G, Thorncroft C (2006) Three dimensional structure and dynamics of African Easterly Waves. part II: dynamical modes. J Atmos Sci 63:2231–2245
Held IM, Suarez MJ (1994) A proposal for the intercomparison of the dynamical cores of atmospheric general circulation models. Bull Am Meteorol Soc 75(10):1825–1830
Horel JD (1982) On the annual cycle of the tropical pacific atmosphere and ocean. Mon Weather Rev 110(12):1863–1878
Hoskins BJ, Simmons AJ (1975) A multi-layer spectral model and the semi-implicit method. Q J R Meteorol Soc 101:637–655
Hsu CPF, Wallace JM (1976) The global distribution of the annual and semiannual cycles in sea level pressure. Mon Weather Rev 104(12):1597–1601
Huang HP, Sardeshmukh PD (2000) Another look at the annual and semiannual cycles of atmosphericangular momentum. J Clim 13(18):3221–3238
Jucker M, Gerber E (2017) Untangling the annual cycle of the tropical tropopause layer with an idealized moist model. J Clim 30(18):7339–7358
Kerr-Munslow A, Norton W (2006) Tropical wave driving of the annual cycle in tropical tropopause temperatures. part i: Ecmwf analyses. J Atmos Sci 63(5):1410–1419
Klinker E, Sardeshmukh PD (1992) The diagnosis of mechanical dissipation in the atmosphere from large-scale balance requirements. J Atmos Sci 49(7):608–627
Leroux S, Hall NMJ (2009) On the relationship between African Easterly Waves and the African Easterly Jet. J Atmos Sci 66:2303–2316
Leroux S, Hall NMJ, Kiladis GN (2011) Intermittent african easterly wave activity in a dry atmospheric model: influence of the extratropics. J Clim 24:5378–5396
Levitus S (1984) Annual cycle of temperature and heat storage in the world ocean. J Phys Oceanogr 14(4):727–746
Lin H, Derome J (1996) Changes in predictability associated with the PNA pattern. Tellus Ser A 48:553-+
Lin H, Derome J, Brunet G (2007) The nonlinear transient atmospheric response to tropical forcing. J Clim 20(22):5642–5665. https://doi.org/10.1175/2007JCLI1383.1
Liu Z (1996) Modeling equatorial annual cycle with a linear coupled model. J Clim 9(10):2376–2385
Marshall J, Molteni F (1993) Toward a dynamical understanding of planetary-scale flow regimes. J Atmos Sci 50:1792–1818
McKinnon KA, Stine AR, Huybers P (2013) The spatial structure of the annual cycle in surface temperature: amplitude, phase, and lagrangian history. J Clim 26(20):7852–7862
Oort AH (1971) The observed annual cycle in the meridional transport of atmospheric energy. J Atmos Sci 28(3):325–339
Oort AH, Vonder Haar TH (1976) On the observed annual cycle in the ocean-atmosphere heat balance over the northern hemisphere. J Phys Oceanogr 6(6):781–800
Peyrillé P, Lafore JP, Boone A (2016) The annual cycle of the west african monsoon in a two-dimensional model: mechanisms of the rain-band migration. Q J R Meteorol Soc 142(696):1473–1489
Roads JO (1987) Predictability in the extended range. J Atmos Sci 44:3495–3527
Sardeshmukh PD, Sura P (2007) Multiscale impacts of variable heating in climate. J Clim 20(23):5677–5695
Schubert S, Chang Y (1996) An objective method for inferring sources of model error. Mon Weather Rev 124(2):325–340
Simmons A, Uppala DD, Kobayashi S (2006) Era-interim: new ecmwf reanalysis products from 1989 onwards. ECMWF Newslett 110:25–36
Sud Y, Walker G, Mehta V, Lau WK (2002) Relative importance of the annual cycles of sea surface temperature and solar irradiance for tropical circulation and precipitation: a climate model simulation study. Earth Interact 6(2):1–32
Thorncroft C, Hall N, Kiladis G (2008) Three dimensional structure and dynamics of African Easterly Waves. Part III: genesis. J Atmos Sci 65:3596–3607
Thorncroft CD, Nguyen H, Zhang C, Peyrille P (2011) Annual cycle of the west african monsoon: regional circulations and associated water vapour transport. Q J R Meteorol Soc 137(654):129–147
Wang B (1994) On the annual cycle in the tropical eastern central pacific. J Clim 7(12):1926–1942
White GH, Wallace JM (1978) The global distribution of the annual and semiannual cycles in surface temperature. Mon Weather Rev 106(6):901–906
Wu Z, Schneider EK, Kirtman BP, Sarachik ES, Huang NE, Tucker CJ (2008) The modulated annual cycle: an alternative reference frame for climate anomalies. Clim Dyn 31(7–8):823–841
Xie SP (1994) On the genesis of the equatorial annual cycle. J Clim 7(12):2008–2013
Yang W, Seager R, Cane MA, Lyon B (2015) The annual cycle of east african precipitation. J Clim 28(6):2385–2404